Areal Seabed Classification using Backscatter Angular Response at 95kHz

J.E. Hughes Clarke [1], B.W. Danforth [2] and P. Valentine [2]

(1): Ocean Mapping Group,
Geodesy and Geomatics Engineering,
University of New Brunswick,
P.O. Box 4400, Fredericton,
N.B., E3B 5A3, CANADA
jhc@omg.unb.ca

(2): Marine and Coastal Geology Program
U.S. Geological Survey,
384 Woods Hole Road,
Woods Hole,
MA 02543-1590, USA
bwd@boomer.er.usgs.gov, pv@nobska.er.usgs.gov

Abstract

A sediment classification scheme is developed based on the angular response (AR) of the seabed backscatter strength. The AR is characterised based on its mean level and slope over predefined angular sectors, and the presence or absence of abrupt changes in slope. Because the AR is derived from a finite area a test is performed to recognise the presence of sediment boundaries. The AR curves are shown to provide improved discrimination over angle invariant methods.

1. Introduction

Seabed backscattered intensity data is now routinely collected as part of regional swath bathymetry surveying. This data, if properly reduced, provides a measure of the seabed backscatter strength as a function of grazing angle (herein termed the angular response (AR)). For a given frequency, the seabed AR represents an inherent property of the seafloor. Traditional low-aspect ratio sidescan surveys, collect most of their useful data at grazing angles in the range 20 to 10 degrees and thus the variation with grazing angle is generally ignored. For a given narrow range of grazing angles, however, a number of quite different seabed types produce similar mean backscatter strengths. Two approaches have been taken to separate these ambiguities. The first is texture [1][2][3], which relies on recognising characteristics of the spatial variance in the backscattered signal. A second is to look at the same seabed through a range of grazing angles to extract the AR [4][5].

The first method has the advantage that the statistics are generally valid irrespective of absolute calibration of the signal level. In contrast, the second method relies on confidence in the absolute level. Recent developments in swath bathymetric surveying have resulted in increased confidence in the received backscatter intensity [6]. Bathymetric swath surveying relies generally on surface mounted systems with a much higher aspect ratio than towed sidescan and thus backscatter data can be easily extracted over a wider range of grazing angles. For the widest swath systems on the market today, grazing angles from vertical to as small as 15 degree or less are now possible allowing one to view the variation in backscatter strength as one (in some cases) passes through the critical angle.

2. Data Acquisition and Handling

2.1 Instrumentation

The sonar used was a Simrad EM1000 [7] multibeam sonar which transmits a 3.3 degree wide (fore-aft) beam over a 150 degree sector at 95 kHz. Sixty roll-stabilised beams are formed over the same angular sector for reception. Received backscattered intensities are compensated for source power, predicted radiation and receive sensitivities, pulse length, ensonified area, spherical spreading and attenuation [8]. The resulting data is first order estimate of the instantaneous backscatter strength. For shallow water operations, a 0.2ms pulse is used and the data is sampled at 5kHz. The sonar is mounted on the NSC Frederick G. Creed and is operated at speeds of about 16 knots. While a swath of 7.4 x the water depth is covered, due to refraction and motion compensation limitations [9] line spacing is normally limited to about 4.5-5.0 x the water depth.

2.2 Location

The dataset used in this study was collected by the Canadian Hydrographic Service on behalf of the United States Geological Survey (USGS). The survey was designed to cover the Stellwagen Bank U.S. National Marine Sanctuary (SBNMS) which extends for over 2,800 square kilometres in water depths ranging from 20 to 200m (Fig. 1). Approximately 80 days of EM1000 data was collected by the USGS over four distinct field survey periods.

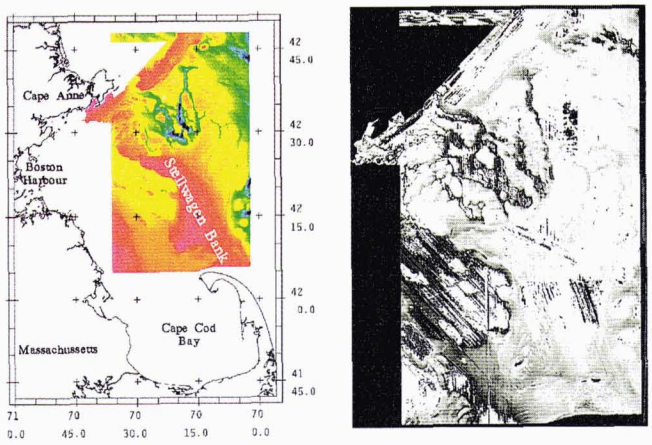

Figure 1:

Left:
Location map showing the relationship of the surveyed area to the region around Boston harbour and Cape Cod. The image is a depth map (blue = 200m, pink = 20m).

The region surveyed extends approximately 70 km N-S and 40 km E-W.

Right:
This is a "normalised" backscatter map for the entire region covered. The grayscale reflects normalised backscatter strength (see text for explanation). Black represents –37.5 dB and white represents –20 dB.

Stellwagen Bank is a shoal ridge extending northward from Cape Cod. It is separated from the cape by an 8 km wide channel herein termed Cape Race Channel. The Bank is exposed to winter storm events from the NE. The sediment on the bank top is known to be actively remobilised during such storm events [11]. The bank terminates abruptly to the west where the bathymetry drops off into the muddy Stellwagen Basin. Seaward of the bank, relict glacial terrains, including glacially scoured boulder and gravel pavements, are common [12]. The bank top and the ramp to seaward are covered with a range of sandy sediments, which are moulded into storm sand ripple fields interspersed with homogenous sand sheets. The Bank has been a rich fishing ground in the past and the modern surface continues to be actively remobilised by a dragger fleet [13]

2.3 Conventional Processing

For the purposes of standard geological mapping a "normalised" backscatter map is generated (Fig. 1). This is an attempt to produce a result comparable to a conventional sidescan mosaic derived from low-aspect ratio towed sidescan sonar (which had previously been the standard mapping instrument for the USGS [10]). Normalisation involves a first attempt at removing the mean variation in backscatter as a function of grazing angle. This is done assuming a lambertian response below 65 degrees grazing and an automatic gain control at higher grazing angles [8]. The aim is to produce a single dimension (normalised backscatter strength) to aid in regional seabed characterisation. This method is sufficient to unambiguously separate the -30 to -40 dB response of the muddy sediments in the basins from the -15 to -25 dB of the coarser sands and gravel from the bank tops (Fig. 1). Such a scheme however, fails when trying to distinguish the wide variety of sand and gravel sediment types that are present on the bank tops and margins. Such materials exhibit little variation in average backscatter strength, yet show obvious physical property differences in cores and bottom photos.

In attempting to distinguish the gravelly sand combinations it was noted that the "normalising" process often failed because the shape of the angular response curve was highly variable. This paper presents a new method, which relies on variations in the shape of the angular response curve as a means of separating lithologies that exhibit similar mean backscatter strengths..

3. Backscatter Data Reduction

3.1 Correcting Radiometric and Geometric Effects.

The EM1000 provides a measure of the instantaneous backscatter strength that has been reduced assuming predicted beam patterns, unrefracted ray paths and a flat seafloor [7][8]. All these assumptions are not strictly correct and additional steps thus have to be taken in order to derive accurate estimates of the true AR.

The EM1000 array has been specifically designed to exhibit uniform radiation and reception sensitivities over the 150 degree angular sector used. In practice, however, there are always +/-2dB variations in the local transmit/receive product

for any particular angular sector. It is thus operationally necessary to estimate these small +/-2dB residuals. The method routinely employed is to find a region of very coarse boulders whose angular response is assumed (from modeling) to be Lambertian, without a strong specular component, and calculate the differences between the observed response and that modeled for all angles. These differences are then subtracted from all other estimates. It is notable that the residuals are observed to be roll insensitive, indicating that the main source of the residuals is not variations in the sensitivity of the physical elements of the array, but variations in the electronics that make up each of the (roll –stabilised) beams.

For the lower grazing angle data the difference in ray path between an ideal straight ray and the refracted ray path may be as much as 3 degrees [9] in strongly downward refracting summer conditions. Fortunately for these surveys all acquisition was performed either in the April or November outside the period when the summer thermocline is developed and thus the effect was not a significant problem.

For regions of strong seabed topography (>2 degrees) it is strictly necessary to estimate the true seabed grazing angles using the local 3D slope of the seafloor derived from the swath bathymetry. Note that the slope is only that exhibited after the bathymetric data cleaning and gridding process and is thus effectively a low-passed filtered version of the true seafloor slope distribution.

3.2 Difficulties at nadir

The near nadir region is in general the hardest place to acquire estimates of the backscatter strength. Conventional sidescan geometries with a broad receive beam merely equate incidence angle with the arccosine of the ratio of time of first arrival and the time of subsequent arrivals. In contrast multibeam sonars extract the backscatter intensity for specific angular sectors from discrete narrow beams. The choice of intensity relies on a good estimate of the slant range to the centre of the beam footprint. Given the amplitude detection methods generally employed (weighted mean time), the estimate may not correspond exactly to the peak in intensity and thus underestimates of the backscatter strength can occur. Another problem that occurs close to normal incidence in the effect of sidelobe interference and subbottom reflections, which both alias the estimate of slant range and contribute to the received intensity, thereby giving false estimates of the backscatter strength.

Prior to 1994 an unrecoverable automatic gain control was applied to all EM1000 backscatter data collected within 25 degrees of vertical incidence [8]. Whilst this was removed in 1994, for the period mid 94 to mid 96, it was clear that the data in this region were being under predicted by about 15dB. A software change in mid 1996 appears to have rectified this problem. As a result the older data (including the first 3 surveys of the SBNMS project) have to be empirically compensated for this. Although seafloor provenance delineation is possible using the near nadir data, the fidelity of the absolute level of the data remain poor. It is presented here, but emphasis is applied to the lower grazing angle data.

3.3 Derivation of mean angular response curves

Because of the stochastic nature of the instantaneously received intensities, it is necessary to average the backscatter strength measurements over a finite time period to come up with a robust estimate of the mean AR. Empirically it was found that 50 ping averages (corresponding to between 100 and 300m forward propagation) were enough to come up with good estimates of the AR curve shape. In addition the data for the full suite of grazing angles has to be acquired from a region extending from nadir to about 3.7 times the water depth to each side (100 to 300m for the range of water depths common on the bank). Thus, as the vessel propagates forward, AR curve estimates are obtained from averaging over two rectangular footprints (of a few 100 metres per side) on either side of the swath (Fig. 2). One therefore runs the risk of averaging over a region of variable seabed character.

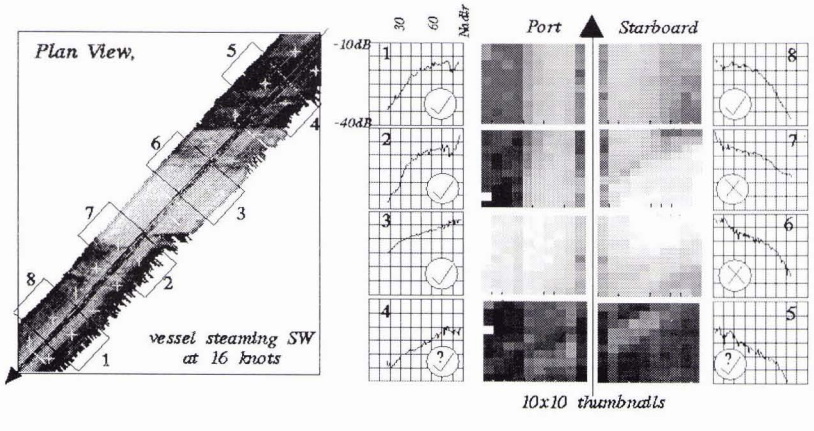

Figure 2: The method of derivation of the 50 ping averages, their corresponding geographic coverage and the method of extracting sidescan "thumbnails" for use in boundary detection (ticks and crosses indicate whether the boundary criteria was met or exceeded).

Whilst for most of the collected data, regions of the scale of the averaging footprint generally appear homogenous in the sidescan imagery, boundaries do occur. Data that is derived over these boundaries is therefore corrupted. In a crude attempt to get around this problem, a 10x10 "thumbnail" image of the seafloor under examination was retained (Fig. 2) for testing purposes. The variance of the averaged intensity distribution in the along track direction only was calculated (in the across track direction, the AR itself will produce a variance). If the variance exceeded a threshold then the angular response curve was rejected.

A result of this approach is that it can only be used to classify homogenous regions on the scale of ½ a swath width or larger. This contrasts markedly with the approach used in deeper water surveys, where commonly the number of survey lines is much lower (as the swaths are much larger), and methods are therefore derived to classify within a single swath [14]. Implicit in the boundary test is a definition of the length scale at which patchy sediment distributions are seen either as a single sediment type or a series of discrete sediment types. For this test, the length scale corresponds to a single pixel, which is 30% of the water depth in size.

4. Parameter Extraction

Early work to invert AR curves for physical properties focussed on the near nadir region to solve for roughness parameters only [15][16][17]. More recent work using EM1000's has focussed on the lower range of grazing angles to attempt full inversion [18]. In all cases the inversion used a single layer seafloor model [19][20]. The inversion assumed that the observed AR curve had no biases due to imperfections in the measurement process (e.g. sections 3.1, 3.2). Because this assumption is invalid for the AR curves herein considered, the focus here has been to extract parameters that adequately describe the salient features of the observed AR curves without being sensitive to small systematic biases.

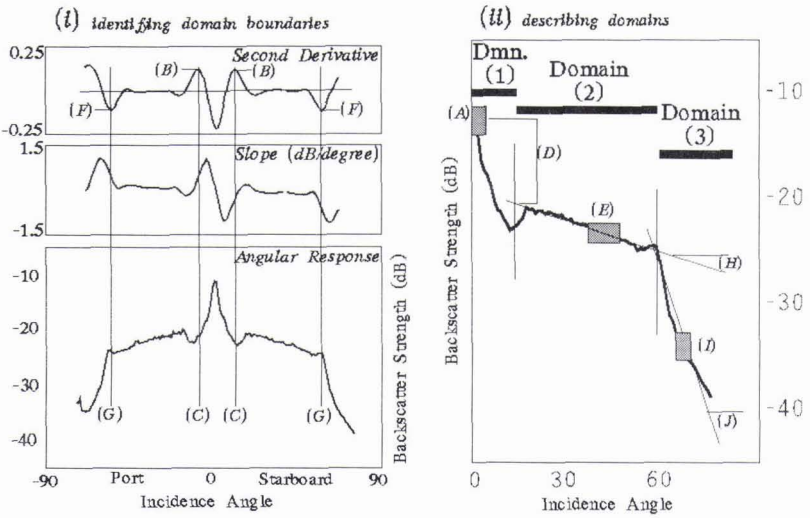

Figure 3: The three main domains of characteristic angular response curves and the parameters extracted to describe the domains

In the application of the model of [19] three main domains within the curve can be easily identified (Fig. 3 zones (1), (2) and (3)). These domains can be clearly seen in the AR curves even with small systematic biases present. Their location and the gross shape of the curve within each domain can be extracted (Fig. 3). The relative importance of the six physical property characteristics used in the single layer fluid model [19] (density and sound speed ratios, spectral strength and exponent, loss tangent and volume scattering) varies as one moves between the three domains. In domains 1 and 2, only the product of the first two terms (which control the impedance contrasts) can be estimated. The boundary between domains 2 and 3 (if visible) in contrast is strongly linked to the sound speed ratio alone (the critical angle effect). The boundary between domains 1 and 2 is most sensitive to the two roughness terms. The volume scattering term is dominant for low impedance sediment in domain 2 but plays little role in domain 3. The roughness terms affect all three domains, but in low impedance sediment they are subordinate to the volume scattering component in domain 2.

The domain boundaries, and the characteristics of the angular response curves within the three domain boundaries can be extracted even in the presence of systematic biases in the data. In this way the important changes in the angular response curves can be reduced to a few parameters that can be used either as a means of empirical classification or even potentially a step toward inversion for seabed physical properties. In addition to parameters describing the shape of the curves, one statistical parameter is used. The coefficient of variance [21] is calculated for narrow angle bins for each 50 ping stack and the average over the range 65-15 degrees grazing is presented.

To illustrate the application of the method, a series of maps are presented (Fig. 4) which show the spatial variation in the parameters over a 30 by 27 km area located on the SE corner of the SBNMS. The different patterns seen in maps A, E

and I illustrate the geographic variation in backscatter strength for three narrow angular subsets of the AR curve. The differences in the 3 maps illustrate that the shape of the AR curves are highly variable. Maps B and F map the confidence with which the domain boundaries are recognised. Maps C and G show the variation in the location of the domain boundaries (note the incoherent pattern in areas where the confidence (expressed in maps B and F) is low). Maps H and J show the spatial variation in the slope of the AR curves for domain 2 and 3 and map D shows the drop in dB in domain 1.

Table 1: description of 12 parameters extracted and the range used in the greyscale spatial maps in Fig. 4.(BS: backscatter strength)

parameter	*description*	*black*	*white*
(A)	Mean BS, 90-85 deg.	-32 dB	-12 dB
(B)	Max. 2nd deriv, (1)-(2) transition	0.02 dB/deg2	0.2 dB/deg2
(C)	Location of (1)-(2) transition	83 deg.	70 deg.
(D)	DB range, domain (1)	-5 dB	10 dB
(E)	Mean BS, 50-40 deg.	-40 dB	-20 dB
(F)	Max. 2nd deriv, (2)-(3) transition	0.0 dB/deg2	0.18 dB/deg2
(G)	Location of (2)-(3) transition	50deg.	15 deg.
(H)	Slope, domain (2)	-0.2 dB/deg	0.0 dB/deg
(I)	Mean BS, 25-20 deg.	-40 dB	-20 dB
(J)	Slope, domain (3)	-1.0 dB/deg	0.0 dB/deg
(K)	Coeff. Variance	0.95	1.0
(L)	Boundary Test Failures	YES	NO

Figure 4: Maps of a 30 by 27 km area (SE section of SBNMS) showing the geographic variation of the 12 parameters described (see table 1, for range used in greyscale).

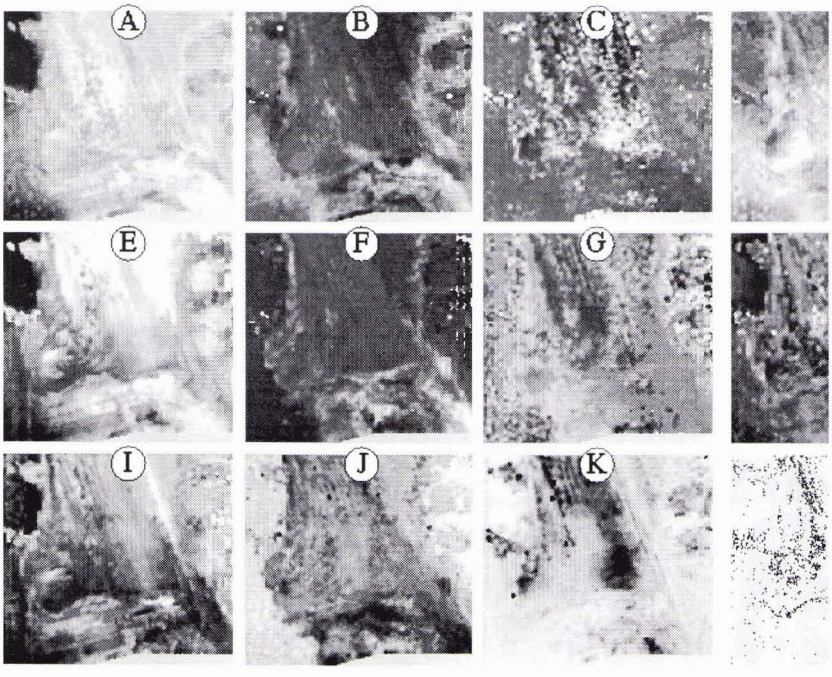

5. GroundTruth Data

While regional historic samples are available [12], the poor positioning confidence of older data and the known temporal variations in the shallow seafloor in this area make their use difficult. More recent, intense sampling programs have been restricted to the southern limit of the bank. This sampling program has consisted of a combination of video imaging, bottom photography and bottom grabs and box cores. Unfortunately for the large fraction the bank which is covered with coarse sediment, sampling limitations (related to the difficulty of recovering statistically significant volumes of coarse sediment in grabs or box cores) have generally resulted in insufficient and unrepresentative samples. Thus descriptions are generally often based on optical imaging only. Grain size is the only commonly available quantitative measurement derived and these data suffer from the aliasing that result when bottom sampling in a spatially heterogeneous area.

6. Characteristic Angular Response Curves

To illustrate the types of AR curves commonly observed within the SBNMS, a representative selection is provided (Fig.'s 5 and 6). All sample curves are derived from acoustic data obtained in the 1994 field season, which was located in the southern area in which the best groundtruth existed. Brief lithologic descriptions are included for all curves, but should be taken as a guide only due to the reasons stated in section 5.

6.1 Stellwagen Bank and Basin

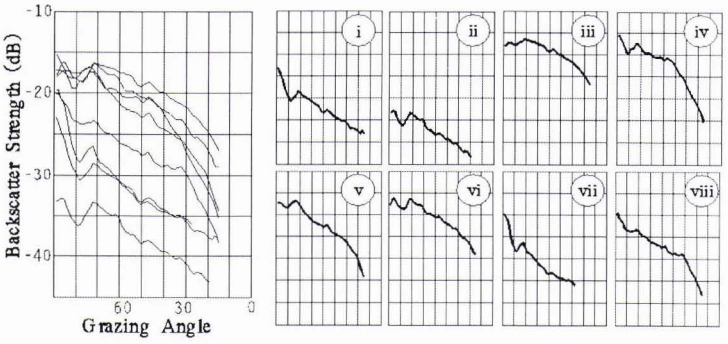

I Silty mud

II Mud

III Cobble pavement

IV Fine sand

V Rippled medium sand, over gravel

VI Boulder fields

VII Sandy mud

VIII Silty sand

Figure 5: Representative AR curves for sediments on Stellwagen Bank and Basin

The AR curves for the sediment on Stellwagen bank and in the basin are similar to those that would be predicted for a single layer model. Lambertian-like AR's are observed for the coarsest sediment (5iii and 5vi) without clear domain boundaries. As expected, for sediments with the lowest sound speed ratios, no domain 3 is observed (5i, 5ii and 5vii). Critical angle effects are seen for sandy sediment (5iv and 5viii).

6.2 Cape Race Channel

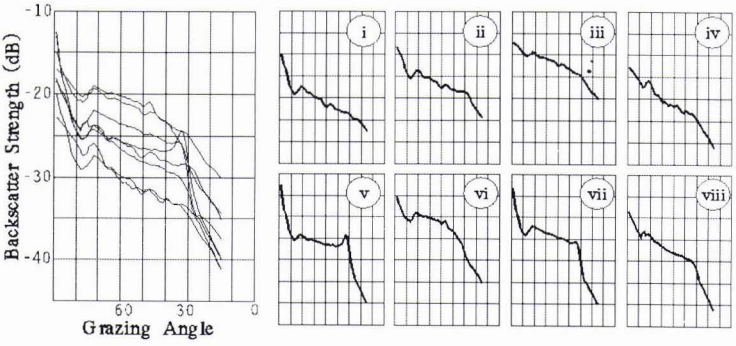

I Silty mud

II Medium sand

III Coarse gravelly sand with cobbles.

IV Clean coarse sand

V Clean medium sand

VI Clean coarse sand overlying gravel

VII Medium sand with pebbles

VIII Medium–coarse sand

Figure 4: Representative AR curves for sediment facies developed in Cape Race channel

In the Cape Race Channel area, critical angle effects are seen throughout (Fig. 6). The location and sharpness of the domain 2-3 boundary is highly variable exhibiting cusps at times (6v and 6vii). In one case (6vi) the location of the critical angle suggests a sound speed ratio of about 1.4 which is far higher than that expected for the surface lithology alone (~1.18) but matches that expected for the underlying layer.. For a number of the sandy sample locations, groundtruth sampling revealed either, interspersed gravel and cobbles, or an underlying layer of gravel.

7 . Discussion on likely physical property controls on observed AR's

Many of the sediments observed in the SBNMS are significantly coarser than those that have been the focus of quantitative acoustic backscatter studies in the past [21][22][23]. Nevertheless they are very representative of the range of coarse facies commonly exhibited on high latitude glaciated continental shelves.

7.1 Explaining the critical angle phenomena observed

While the limitations (outlined in Section 3.2) of the measurement of the AR preclude the confident use of the curves for inversion (note the prevalent depression in all the curves at ~75-80 grazing). The shape, and more particularly the change in shape, of the angular response curves between common lithologies may be compared to predictions for material of similar physical properties. For the case of a single layer seafloor type [19][20], critical angle effects would be expected in sediments in which the sediment/seawater sound speed ratio exceeds ~1.04. For this simple case, the location of the inflection is unique indicator of the sediment sound speed. Two end member cases are recognised: a cusp for cases in which surface roughness is dominant (Fig. 6v), and a step function for the case where volume scattering is terminated (Fig 6viii). A break in slope would not be obvious for the rougher, higher impedance sediment types with no volume contribution (Fig. 5iii and vi) or for softer sediment with a sediment/seawater velocity ratio of less than 1.04 (Figs 5I,,ii and vii, 6i). We find, however, that while models such as [19] can predict the presence of the inflection, they cannot reproduce the rapid drop off below the critical angle sometimes observed(Fig. 6v, 6vii). Also in some cases (Fig. 5iv and Fig. 6vi) the predicted surface sound speed, often in the range ~1900-2000m/s, is too high for typical medium and coarse sands.

Alternate explanations are thus needed. More recent models that include the effect of shallow gradients, layering and shear in the shallow subsurface [24][25] are examined. For the case of a surface sediment layer of less than a wavelength in depth it has been shown [24] that the critical angle often reflects the velocity contrast of the lower (higher velocity layer). With the introduction of shear in the lower layer, the drop off in backscatter beyond the critical angle is notably steeper than that which would be exhibited for the upper layer alone [24]. These two results allow us to better match the observed curves. These, together with field evidence of a discontinuously buried higher backscatter layer (revealed in bottom photos, samples and deep-tow sidescan images) support the idea of a thin surface layer. For this case, the apparent volume scattered phenomena may either be volume scattering from the upper layer or scattering from the partly buried interface.

8. Conclusions

With appropriate data reduction, estimates of the seabed backscatter angular response can be routinely derived from calibrated multibeam echosounders. In the water depths considered (20-200m), to do so requires that there be spatially homogenous regions of the seafloor a few hundred metres wide. Parameters describing the shape of the angular response curve allow improved sediment boundary discrimination in regions where mean backscatter strength is almost constant. The shape of the curve below 40 degrees is especially revealing as the response in the vicinity of the critical angle may be observed. Curve parameterisation allows the potential to invert for seabed physical properties. The success of the inversion, however, is dependent on both the fidelity of the measurements and the appropriateness of the model used.

For a number of the examples presented, comparison of observed angular responses to the results obtained assuming a single layer model suggests that such a simple model is often not valid. An improved fit may be obtained by incorporating more recent models [24][25] that account for shear, gradients and layering in the shallow subsurface (< a few wavelengths ~1-3cm). Limited groundtruth observations support this with evidence of discontinuous surface layers of finer grained sandy sediment over a coarse-grained gravel pavement.

While confident remote sediment classification remains an elusive goal, the routine availability of near-quantitative angular response measurements provides an additional means of seabed discrimination . Used together with other methods such as normal incidence and textural methods, angular response methods can provide an improvement in underway sediment classification.

Acknowledgements

Funding for the SBNMS surveys was provided through the US National Marine Sanctuary Program and the USGS Coastal Marine Geology Program. This research was funded through the NSERC Industrial Research Chair in Ocean Mapping. We are indebted to the officers and crew of the NSC Frederick G. Creed, and greatly appreciate the assistance of Richard Sanfacon (CHS) , Vee-Ann Cross, Jane Denny and Erik Schmuck (USGS).

References

[1] Pace, N.G. and Gao, H., 1988, Swathe seabed classification: IEEE J. Oc. Eng., v.13, p. 83-90.
[2] Reed, T.B. and Hussong, D. , 1989, Digital image processing techniques for enhancement and classiication of SeaMARC II side scan sonar imagery: JGR, v.84, B6, p.7469-7490.
[3] Blondel, P., 1996, Segmentation of the Mid-Atlantic Ridge south of the Azones, based on acoustic classification of TOBI data: in Geol. Soc. Spec. Pub. no. 118, p.17-28.
[4] de Moustier, C. and Alexandrou, D., 1991, Angular dependence of 12 kHz seafloor acoustic backscatter: JASA, v.90, p.522-531.
[5] Hughes Clarke, J.E., 1994, Toward remote seafloor classification using the angular response of acoustic backscattering: a case study from multiple overlapping GLORIA data: IEEE Journal of Oceanic Engineering v.19, no.1, p.364-374.
[6] Hughes Clarke, J.E, 1993, The potential for seabed classification using backscatter from shallow water multibeam sonars, in Pace, N. and Langhorne, D.N., Proc. of the Inst. of Acoustics, v. 15, pt. 2, p. 381- 388.
[7] Simrad, 1992, SIMRAD EM1000, Hydrographic echo sounder, Product Description: Simrad Subsea A/S, #P2415E.
[8] Hammerstad E., 1994, Backscattering and Sonar Image Reflectivity: EM12/950/1000 Technical Note, 10p.
[9] Hughes Clarke, J.E., Mayer, L.A. and Wells, D.E., 1996, Shallow-water imaging multibeam sonars: A new tool for investigating seafloor processes in the coastal zone and on the continental shelf: MGR, v.18, p.607-629.
[10] Danforth,W.C., O'Brien, T.F. and Schwab, W.C., 1991, Near-realtime mosaics from high-resolution sonar: Sea Technology, v.32, no. 1, p.54-59.
[11] Valentine, P.C., and Schmuck, E.A., 1993, Storm-driven sediment transport on Stellwagen Bank, Gulf of Maine region (abs.): Geological Society of America Abstracts with Programs, v. 25, no. 6, p. A379-380.
[12] Schlee,J.D., Folger,D.W. and O'Hara, C.J., 1973, Bottom Sediments on the continental shelf off the Northeastern United States, Cape Cod to Cape Ann, Massachussetts: USGS .Misc. Geologic Investigations, ap I-746.
[13] Auster, P.J., Malatesta, R.J., Langton, R.W., Watling, L., Valentine, P.C., et al., 1996, The impacts of mobile fishing gear on low topography benthic habitats in the Gulf of Maine (northwest Atlantic): implications for conservation of fish populations: Reviews in Fisheries Science, v. 4, no. 2, p. 185-202 .
[14] Dugelay, S., Graffigne, C. and JM. Augustin, 1996, Deep seafloor characterisation with multibeam echosounders by image segmentation using angular acoustic variations: Proceedings SPIE, Denver.
[15] Matsumoto, H., Dziak, R.P. and Fox, C., 1993, Estimation of seafloor microtopographic roughness through modeling of acoustic backscatter data recorded by multibeam systems: JASA v.94, p.2776-2787.
[16] Michalopoulu, Z-H, Alexandrou, D. and deMoustier, C., 1994, Application of a maximum likelihood processor to acoustic backscatter for the estimation of the seafloor roughness parameters: JASA, v.95, p.2467-2477.
[17] Michalopoulu, Z-H and Alexandrou, D., 1996, Bayesian modeling of acoustic signals for seafloor identification: JASA v.99, 223-233.
[18] Gott, R.M., 1995, Seafloor characterization using multibeam sonar amd acoustic backscatter modeling: PhD thesis, Tulane University.
[19] Jackson, D.R., Winebrenner, D.P. and Ishimaru, A., 1986, Application of the composite roughness model to high-frequency bottom backscattering: JASA, v.79, p.1410-1422.
[20] Mourad P.D. and Jackson, D.R., 1989, High frequency sonar equation models for bottom backscatter and forward loss: Proc. OCEANS'89, v.IV, p.1168-1175.
[21] Stanic, S., Briggs, K.B., Fleischer, Sawyer,W.B. and Ray, R.I., 1989, High frequency acoustic backscattering from a coarse shell ocean bottom: JASA, v.85, p.125-136.
[22] Jackson, D.R., Baird, A.M., Crisp, J.J. and Thomson, P.A.G., 1986, High-frequency bottom backscatter measurements in shallow water: JASA, v.80, p.1188-1199.
[23] Jackson, D.R. amd Briggs, K.B., 1992, High frequency bottom backscattering: Roughness versus sediment volume scattering: JASA, v.92, p.962-977.
[24] Essen, H.-H., 1994, Scattering from a rough sedimental seafloor containing shear and layering: JASA, v.95, p.1299-1310.
[25] Moe, J.E. and Jackson, D.R., 1994, First-order perturbation solution for rough surface scattering cross section including the effects of gradients: JASA, v.96, p.1747-1754.